Journal of Computers Vol. 34 No. 6, December 2023, pp. 91-105
doi: 10.53106/199115992023123406007

Modified Harris Hawks Optimization Algorithm with Multi-strategy for Global Optimization Problem

Cui-Cui Cai[1], Mao-Sheng Fu[1], Xian-Meng Meng[2*], Qi-Jian Wang[2], Yue-Qin Wang[2]

[1] College of Electronics and Information Engineering, West Anhui University, Lu'an 237012, China
03000083@wxc.edu.cn, fumaosheng@wxc.edu.cn

[2] College of Electronics Engineering, Anhui Xinhua University, Hefei 230088, China
mengxianmeng@axhu.edu.cn, wangqijian@axhu.edu.cn, wangyueqin@axhu.edu.cn

Received 30 June 2022; Revised 1 July 2022; Accepted 1 July 2022

Abstract. As a novel metaheuristic algorithm, the Harris Hawks Optimization (HHO) algorithm has excellent search capability. Similar to other metaheuristic algorithms, the HHO algorithm has low convergence accuracy and easily traps in local optimal when dealing with complex optimization problems. A modified Harris Hawks optimization (MHHO) algorithm with multiple strategies is presented to overcome this defect. First, chaotic mapping is used for population initialization to select an appropriate initiation position. Then, a novel nonlinear escape energy update strategy is presented to control the transformation of the algorithm phase. Finally, a nonlinear control strategy is implemented to further improve the algorithm's efficiency. The experimental results on benchmark functions indicate that the performance of the MHHO algorithm outperforms other algorithms. In addition, to validate the performance of the MHHO algorithm in solving engineering problems, the proposed algorithm is applied to an indoor visible light positioning system, and the results show that the high precision positioning of the MHHO algorithm is obtained.

Keywords: swarm intelligence algorithm, modified Harris Hawks Optimization, chaotic mapping, nonlinear control strategy, visible light positioning

1 Introduction

Nowadays, optimization problems have been widespread in many fields, such as computing science, data analytics, automatic control, and engineering design [1-6]. Due to the nonlinear and constrained characteristics of these problems, it is extremely difficult to resolve some classes of problems with traditional mathematical optimization algorithms. Accordingly, metaheuristic algorithms have addressed many problems as efficient solutions due to their simple principle and easy implementation. In addition, the algorithms have the advantages of avoiding local optimal and do not require gradient information.

In general, there are two types of metaheuristic algorithms: swarm intelligence algorithms and evolutionary algorithms. Evolutionary algorithms are supported by evolutionary ideas and modeled on biological evolutionary mechanisms in nature. This type of metaheuristic algorithm is mainly Genetic Algorithms (GA) [7], Differential Evolution (DE) [8], and Biogeography-based Optimization (BBO) algorithm [9]. Swarm intelligence algorithms are designed to emulate group behavior in nature. The decentralized, collective, and self-organized cooperative behavior between individuals in swarms is coordinated in these algorithms to overcome the problem of an optimization process. In nature, swarm intelligence algorithms produce multiple solutions randomly and improve them throughout the search of the algorithm. This type of metaheuristic algorithm is mainly Particle Swarm Optimization (PSO) [10], Ant Colony Optimization (ACO) [11], Cuckoo Search (CS) Algorithm [12], Gray Wolf Optimizer (GWO) [13], Bat Algorithm (BA) [14], Whale Optimization Algorithm (WOA) [15], Marine Predators Algorithm (MPA) [16], and Sparrow Search Algorithm (SSA) [17].

Harris hawks optimization (HHO) is a novel metaheuristic algorithm presented in 2019, which is inspired by the cooperative behavior of Harris Hawks in hunting escaping prey [18]. The HHO algorithm consists of an exploration phase and an exploitation phase, and the global optimal solution can be searched quickly by transforming the algorithm phase. Meanwhile, the HHO algorithm has been applied to many fields due to its excellent search and execution capabilities. For example, Çetinbaş et al. [19] employed the HHO algorithm to optimize

* Corresponding Author

and design the autonomous AC grid for commercial loads. Akdag et al. [20] presented a modifying HHO algorithm with a random distribution function definition, and the performed scheme was used to optimize the power flow optimum. Du et al. [21] presented a hybrid HHO model for the air pollutant prediction, and the superiority of the model prediction performance was verified. Chen et al. [22] developed an enhanced HHO algorithm combined with chaotic searching and opposition-based learning to address the problem of photovoltaic models. The proposed algorithm can estimate the critical parameters of photovoltaic models with high accuracy.

According to the aforementioned literature, the excellent search performance of the HHO algorithm has been proven. However, the HHO algorithm requires some improvements when solving complex optimization problems. This is because the HHO algorithm, like most optimization algorithms, has low convergence accuracy and easily traps in a local optimum.

To conquer the inherent weaknesses of the HHO algorithm, many improved HHO algorithms are proposed to resolve optimization problems. Bao et al. [23] developed a hybrid HHO algorithm with DE algorithm for multilevel thresholding image segmentation. Attiya et al. [24] proposed a modified HHO (MHHO) algorithm based on simulated annealing for scheduling jobs. Li et al. [25] developed an enhanced Harris Hawk algorithm with two novel strategies to optimize the practical design problems. All these modified algorithms can effectively improve the search performance of the HHO algorithm, however, the complexity of the algorithm is significantly increased.

This paper presents a new MHHO algorithm with less algorithmic complexity increasing. At the initialization of the algorithm, chaotic mapping is employed for the population initialization, which promotes the HHO algorithm to choose an appropriate initiation position. In addition, a nonlinear update of escape energy is presented to control the phase transition of the algorithm, which makes the algorithm avoid falling into a local optimum. Moreover, a nonlinear control strategy is applied to the optimization process, which further enhances the algorithm's efficiency.

Therefore, this paper aims to enhance the search efficiency of the HHO algorithm and use it for solving the practical problem of indoor visible light positioning (VLP) [26, 27]. The main contributions of this paper are formulated as follows:

- Chaotic mapping is utilized for the population initialization in the HHO algorithm, which updates the random initialized positions and selects an appropriate initiation position for the algorithm.
- To improve the search performance of the HHO algorithm, a nonlinear update of escape energy and a nonlinear control strategy is proposed for the MHHO algorithm.
- The optimization problem of indoor VLP is introduced, the MHHO algorithm is used to address the problem, and the positioning accuracy of the indoor VLP system has been effectively improved.

The remainder of the paper is structured as follows. Sect. 2 briefly depicts the principle of the HHO algorithm. The MHHO algorithm is described in Sect. 3. The experimental results are analyzed and discussed in Sect. 4. Finally, Sect. 5 concludes this paper.

2 HHO Algorithm

As a novel metaheuristic algorithm, the HHO algorithm mimics the natural process of Harris Hawks in cooperatively hunting prey. The HHO algorithm has been used for several applications because of its excellent search capability and few control parameters [18, 28]. HHO algorithm employs two stages to update the positions of hawks: the exploration stage and the exploitation stage. The specific stages of the HHO algorithm are depicted as follows.

2.1 Exploration Phase

During this phase, Harris hawks are randomly scattered to prey-hunting locations employing two exploration approaches. One approach is that Harris hawks perch in an area close to the prey's location, the other approach is that the Harris hawks wait randomly in tall trees. The two methods are implemented equally and can be represented as:

$$X(t+1)=\begin{cases} X_{rand}(t)-r_1\left|X_{rand}(t)-2r_2X(t)\right|, & q\geq 0.5 \\ (X_{rabbit}(t)-X_m(t))-r_3(LB+r_4(UB-LB)), & q<0.5 \end{cases}, \quad (1)$$

$$X_m(t)=\frac{1}{N}\sum_{i=1}^{N}X_i(t), \quad (2)$$

where $X(t+1)$ and $X(t)$ denote the hawk's position vector for the next iteration and the current iteration, respectively. $X_{rand}(t)$ denotes a randomly selected position vector, $X_{rabbit}(t)$ represents the best position vector in each iteration, $X_m(t)$ indicates the hawk's average location, LB and UB represent the upper and lower bounds of the solution space, respectively. q, r_1, r_2, r_3, and r_4 are the random variables in (0,1), and N is the total number of hawks.

2.2 Transition Phase

The phase transition of the HHO algorithm relies mainly on the prey's escape energy. The Harris Hawk moves to the exploration phase when the exploration phase is completed. The energy of the prey escaping E is calculated as:

$$E=2E_0(1-t/T), \quad (3)$$

where E_0 represents the initial escape energy randomly generated in [-1,1], t and T are the current iteration number and the maximum iteration number, respectively.

2.3 Exploitation Phase

During this phase, the Harris hawks will attack the rabbit after completing the encirclement of the prey, and the actual scenarios are extremely complicated. As a result, four strategies are used to simulate the actual situation of Harris Hawk hunting according to the probability of prey escaping r and the E.

Soft Besiege ($r \geq 0.5$ and $E \geq 0.5$). In this strategy, the rabbit still has enough energy. Therefore, the hawks surround the rabbit so that it loses more energy, and then makes a sudden pounce. The process can be expressed as:

$$X(t+1)=\Delta X(t)-E\left|JX_{rabbit}(t)-X(t)\right|, \quad (4)$$

$$\Delta X(t)=X_{rabbit}(t)-X(t), \quad (5)$$

$$J=2(1-r_5), \quad (6)$$

where $\Delta X(t)$ represents the difference location vector, J denotes the rabbit's jumping strength, and r_5 is a random variable.

Hard Besiege ($r \geq 0.5$ and $E < 0.5$). In this strategy, the rabbit consumes so much energy that it does not have sufficient energy to escape. The hawks make the final surprise pounce without surrounding the rabbit. The process is given by:

$$X(t+1)=X_{rabbit}(t)-E\left|\Delta X(t)\right|. \quad (7)$$

Soft Besiege with Progressive Rapid Dives ($r < 0.5$ and $E \geq 0.5$). For this strategy, the rabbit remains sufficient energy to escape from the capture. Harris Hawk requires to carry out a soft siege as usual, then preys suddenly on

the rabbit. The process can be formulated as:

$$Y = X_{rabbit}(t) - E\left|JX_{rabbit}(t) - X(t)\right|. \tag{8}$$

If the situation is inappropriate, hawks will suddenly dive for the prey. The Levy flight mechanism is applied to this case. This situation can be given by:

$$Z = Y + S \times LF(D), \tag{9}$$

where S is a randomly generated vector, D denotes the dimension, and LF indicates the Levy flight that can be calculated as:

$$LF(x) = 0.01 \times \frac{\mu \times \sigma}{\left|\nu\right|^{1/\beta}} (\beta = 1.5), \tag{10}$$

$$\sigma = \left(\frac{\Gamma(1+\beta) \times \sin(\pi\beta/2)}{\Gamma(\frac{1+\beta}{2}) \times \beta \times 2^{(\frac{\beta-1}{2})}}\right), \tag{11}$$

where μ and v are random numbers, and Γ denotes the gamma function.

Therefore, the Harris hawk position updating of the soft besiege phase can be formulated as:

$$X(t+1) = \begin{cases} Y, if\ Fitness(Y) < Fitness(Z) \\ Z, if\ Fitness(Y) > Fitness(Z) \end{cases}, \tag{12}$$

where *Fitness* represents the fitness function.

Hard Besiege with Progressive Rapid Dives (r < 0.5 and E < 0.5). For this strategy, the prey's energy was almost exhausted and could not support the escape. The Harris Hawks form a solid siege before the surprise attack and attempt to shorten the distance from the rabbit. The above process can be formulated as:

$$X(t+1) = \begin{cases} Y, if\ Fitness(Y) < Fitness(Z) \\ Z, if\ Fitness(Y) > Fitness(Z) \end{cases}, \tag{13}$$

where Y and Z are calculated as:

$$Y = X_{rabbit}(t) - E\left|JX_{rabbit}(t) - X_m(t)\right|, \tag{14}$$

$$Z = Y + S \times LF(D). \tag{15}$$

3 Modified Harris Hawks Optimization Algorithm

In recent research, it has been demonstrated that the HHO algorithm has excellent search capability. Similar to other metaheuristic algorithms, the HHO algorithm is easily trapped in a local optimum when dealing with complex optimization problems [29, 30]. However, to overcome the shortcoming of the algorithm, a novel MHHO with a multi-strategy is proposed in this section.

3.1 Chaotic Mapping

Chaotic mapping is a complex dynamic behavior of the nonlinear system and has been applied to intelligent optimization algorithms [31-33]. Chaotic mapping is applied to population initialization to select appropriate initiation positions, which improves the searching efficiency of the optimization algorithm.

The common chaotic mapping mainly includes Logistic mapping, Tent mapping, and Iterative mapping. The Iterative mapping is used for the population initialization of the MHHO algorithm, which can be expressed as:

$$x_t^{'} = \sin(a\pi / x_t) , \tag{16}$$

where x_t is the position vectors before the update, $x_t^{'}$ is the updated position vectors, and a is the control parameter in (0,1).

3.2 Nonlinear Escape Energy Update Strategy

The energy of prey E is an important essential concept in HHO and is employed to control the transition of the phases [28]. Due to the linear decrease of E1, the algorithm easily falls into a local optimum in the first half of the iteration. To promote the capability of the HHO algorithm, the prey escaping energy E with a nonlinear updating strategy is presented, denoted as:

$$E=2E_0e^{-t/T} . \tag{17}$$

The representation of prey escape energy in HHO and MHHO is shown in Fig. 1.

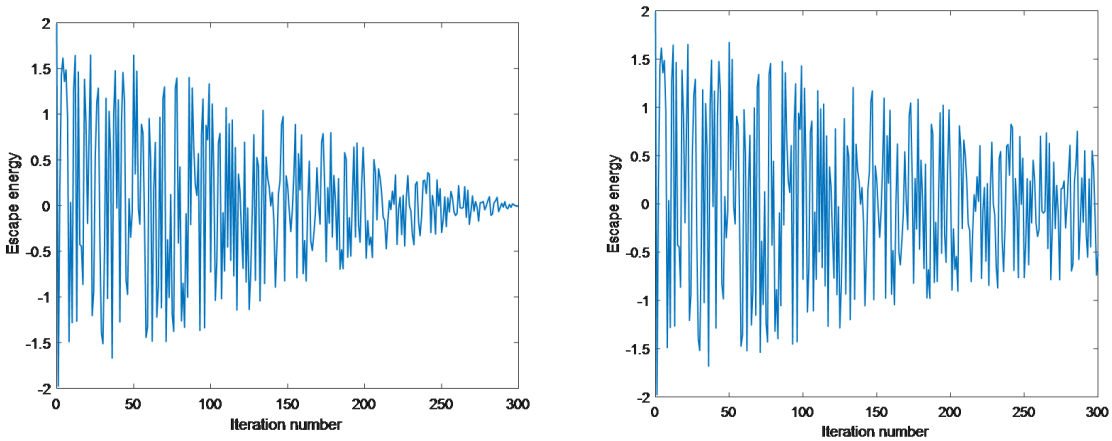

(a) HHO (b) MHHO

Fig. 1. Representation of prey escape energy in HHO and MHHO

3.3 Nonlinear Control Strategy

In the HHO algorithm, the efficiency of the different stages is affected by the variety of potential solutions. The use of nonlinear escape energy enhances the search efficiency, however, a nonlinear control parameter is also applied to further enhance the efficiency of the HHO algorithm. The control parameter ω is given by [34]:

$$\omega=2e^{-(8t/T)^2} . \tag{18}$$

Then, in the soft besieging progressive dives, Eq. (8) and Eq. (9) are modified as follows:

$$Y = \omega \cdot X_{rabbit}(t) - E\left|JX_{rabbit}(t) - X(t)\right|, \tag{19}$$

$$Z = \omega \cdot Y + S \times LF(D). \tag{20}$$

Moreover, Eq. (14) and Eq. (15) are modified as follows:

$$Y = \omega \cdot X_{rabbit}(t) - E\left|JX_{rabbit}(t) - X_m(t)\right|, \tag{21}$$

$$Z = \omega \cdot Y + S \times LF(D). \tag{22}$$

The HHO algorithm combined with chaotic mapping, nonlinear controlling, and nonlinear escape energy strategies is proposed to improve the searching performance. Fig. 2 shows the flowchart of the MHHO algorithm.

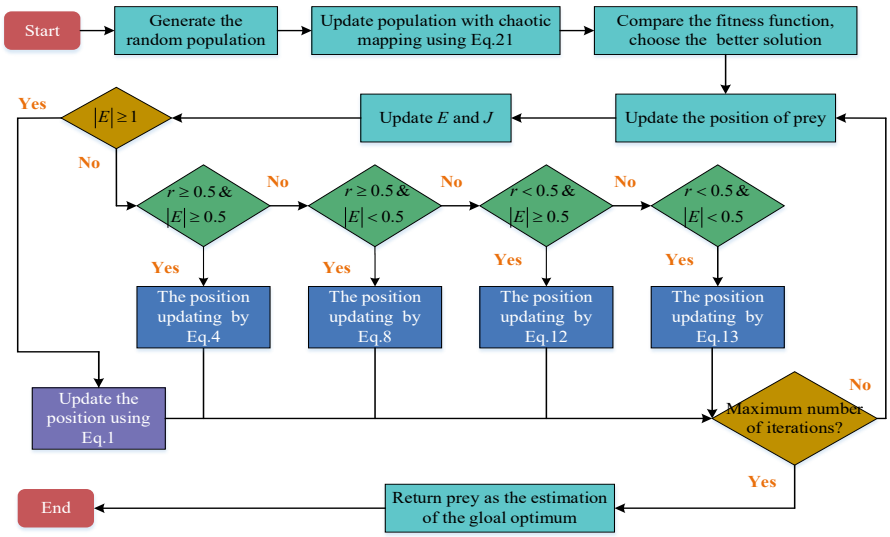

Fig. 2. Flowchart of the MHHO algorithm

4 Performance Evaluation and Analysis

4.1 Test Functions and Experiment Settings

To demonstrate the efficiency of the MHHO algorithm, the benchmark functions (F1~F13) [35, 36] are used to perform optimization experiments. In addition, five meta-heuristic algorithms (GWO [13], WOA [15], MPA [16], SSA [17], HHO [15]) also perform the same experiments. Owing to the certain randomness of the algorithmic search, each experiment was repeated ten times separately for testing. Table 1 lists the information on the benchmark functions.

Table 1. Benchmark test functions

Function	*Dim*	Range	f_{min}
$F_1(x)=\sum_{i=1}^{N}x_i^2$	30	[-100,100]	0
$F_1(x)=\sum_{i=1}^{N}\lvert x_i\rvert+\prod_{i=1}^{N}\lvert x_i\rvert$	30	[-10,10]	0
$F_3(x)=\sum_{i=1}^{N}(\sum_{j=1}^{i}x_j)$	30	[-100,100]	0
$F_4(x)=\max_i\{\lvert x_i\rvert,1\le i\le N\}$	30	[-100,100]	0
$F_5(x)=\sum_{i=1}^{N}[100(x_{i+1}-x_i^2)^2+(x_i-1)^2]$	30	[-30,30]	0
$F_6(x)=\sum_{i=1}^{N}(\lvert x_i+0.5\rvert)^2$	30	[-100,100]	0
$F_7(x)=\sum_{i=1}^{N}ix_i^4+random[0,1]$	30	[-1.28,1.28]	0
$F_8(x)=\sum_{i=1}^{N}-x_i\sin(\sqrt{\lvert x_i\rvert})$	30	[-500,500]	-418.9829×*Dim*
$F_9(x)=\sum_{i=1}^{N}[x_i^2-10\cos(2\pi x_i)+10]$	30	[-5.12,5.12]	0
$F_{10}(x)=-20\exp(-0.2\sqrt{\frac{1}{n}\sum_{i=1}^{N}x_i^2})-\exp(\frac{1}{n}\sum_{i=1}^{N}\cos(2\pi x_i)+20+e$	30	[-32,32]	0
$F_{11}(x)=\frac{1}{4000}\sum_{i=1}^{N}x_i^2-\prod_{i=1}^{N}\cos(\frac{x_i}{\sqrt{i}})+1$	30	[-600,600]	0
$F_{12}(x)=\frac{\pi}{n}\{10\sin(\pi y_1)+\sum_{i=1}^{N-1}(y_i-1)^2[1+\sin^2(\pi y_{i+1})+(y_n-1)^2]\}+\sum_{i=1}^{N}u(x_i,10,100,4)$, $y_i=1+\frac{x_i+1}{4}$, $u(x_i,a,k,m)=\begin{cases}k(x_i-a)^m, x_i>a\\0,-a<x_i<a\\k(-x_i-a)^m, x_i<-a\end{cases}$	30	[-50,50]	0
$F_{13}(x)=0.1\{\sin^2(3\pi x_1)+\sum_{i=1}^{N}(x_i-1)^2[1+\sin^2(3\pi x_1)]+(x_n-1)^2[1+\sin^2(3\pi x_1)]\}+\sum_{i=1}^{N}u(x_i,5,100,4)$	30	[-50,50]	0

4.2 Analysis of Experimental Results

In this simulation experiment, the maximum number of iterations is 500, and the population size is 20. The convergence curves of F1~F13 functions with different algorithms are shown in Fig. 3, and the optimal values obtained for F1~F13 are shown in Table 2.

Table 2. Results of benchmark functions

Function		GWO	WOA	MPA	SSA	HHO	MHHO
F1	AVG	1.8867E-23	2.0565E-63	3.0778E-23	9.3417E-04	6.9432E-92	**3.6734E-157**
	STD	2.2181E-23	5.6460E-63	4.3377E-23	1.0303E-03	2.1841E-91	**0.0000E+00**
F2	AVG	3.9047E-14	1.2501E-48	5.4616E-13	5.0001E+01	3.7143E-51	**4.5907E-81**
	STD	2.3816E-14	2.3811E-48	5.5906E-13	1.9437E+01	6.3715E-51	**8.5383E-81**
F3	AVG	1.3963E-03	5.8345E+04	2.8709E-04	2.7285E+04	5.6910E-64	**9.2837E-141**
	STD	2.6246E-03	1.5002E+04	4.1802E-04	5.9999E+03	1.6970E-63	**2.9358E-140**
F4	AVG	9.4296E-06	5.1402E+01	3.3386E-09	6.8802E+01	6.5657E-48	**2.2544E-76**
	STD	1.0878E-05	2.9082E+01	1.5885E-09	1.4550E+01	2.0650E-47	**5.8689E-76**

F5	AVG	2.7206E+01	2.8165E+01	2.5858E+01	2.7773E+04	2.9131E-02	7.7705E-03
	STD	6.1194E-01	5.0853E-01	4.4838E-01	4.2985E+04	3.1792E-02	1.7685E-02
F6	AVG	1.0852E+00	1.1022E+00	2.7504E-02	1.1162E-03	5.5310E-04	**3.0587E-06**
	STD	2.9540E-01	4.6745E-01	5.8022E-02	1.3073E-03	3.2034E-04	**3.4268E-06**
F7	AVG	2.6023E-03	5.8587E-03	1.3789E-03	4.7709E+00	2.8475E-04	**3.5304E-05**
	STD	9.4450E-04	4.5450E-03	4.9037E-04	1.1628E+01	2.3588E-04	**2.6120E-05**
F8	AVG	-5.2314E+03	-9.0149E+03	-8.5559E+03	-8.8653E+03	-1.0031E+04	-1.2568E+04
	STD	1.1744E+03	1.8682E+03	2.8378E+02	4.1444E+02	7.9407E+03	1.6572E+00
F9	AVG	2.7244E+00	5.6843E-15	0.0000E+00	1.6120E+02	0.0000E+00	0.0000E+00
	STD	2.1292E+00	1.7975E-14	0.0000E+00	3.5997E+01	0.0000E+00	0.0000E+00
F10	AVG	8.6065E-13	4.4409E-15	1.3658E-12	1.2475E+01	8.8818E-16	8.8818E-16
	STD	3.5572E-13	2.9008E-15	1.2241E-12	7.5799E+00	0.0000E+00	0.0000E+00
F11	AVG	2.2204E-16	1.5522E-02	0.0000E+00	2.4898E-02	0.0000E+00	0.0000E+00
	STD	7.0215E-16	4.9085E-02	0.0000E+00	2.8532E-02	0.0000E+00	0.0000E+00
F12	AVG	8.6936E-02	5.2355E-02	2.1988E-03	3.8553E+00	2.0455E-05	**1.4042E-06**
	STD	5.3540E-02	2.8503E-02	2.2822E-03	2.5484E+00	2.7183E-05	**2.4632E-06**
F13	AVG	1.0627E+00	9.4915E-01	1.0709E-01	5.0531E+00	2.9987E-04	**2.9481E-06**
	STD	2.2168E-01	2.7599E-01	1.1676E-01	5.6815E+00	3.9704E-04	**3.4576E-06**

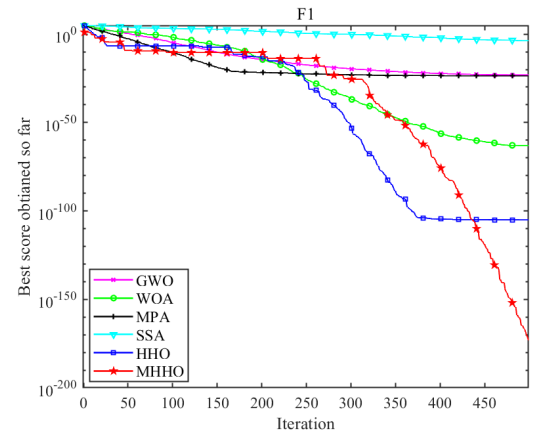

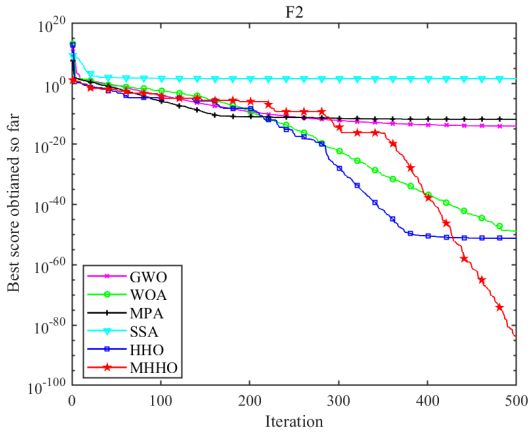

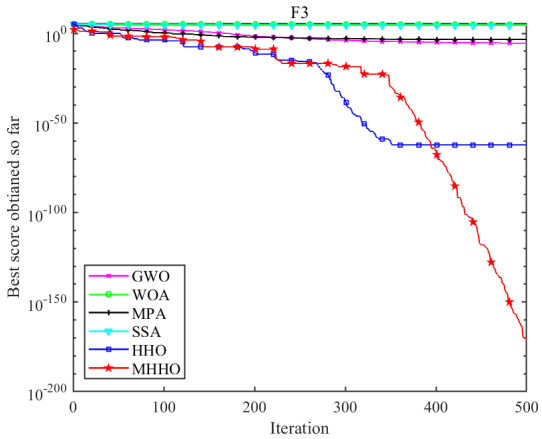

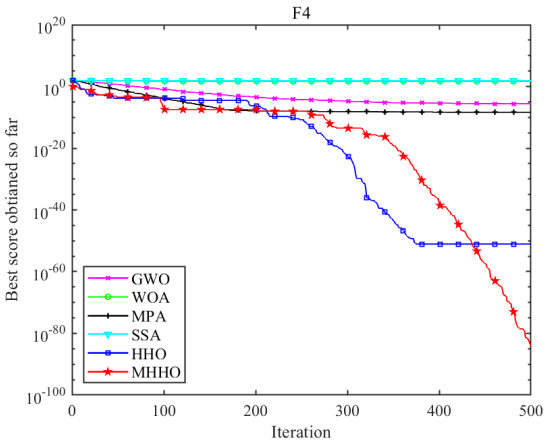

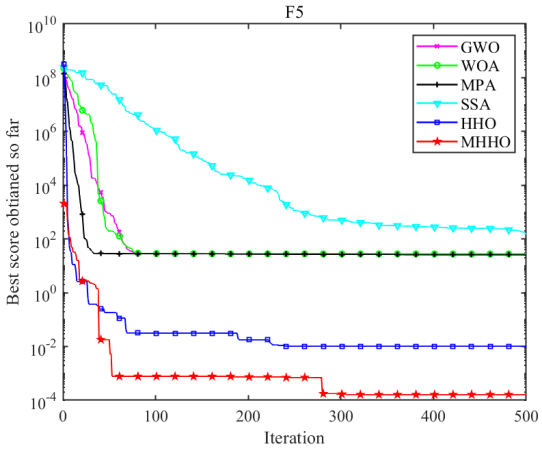
F5
Best score obtianed so far
Iteration
GWO
WOA
MPA
SSA
HHO
MHHO

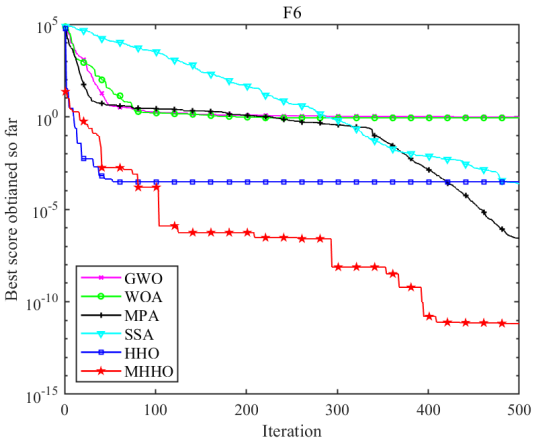
F6
Best score obtianed so far
Iteration
GWO
WOA
MPA
SSA
HHO
MHHO

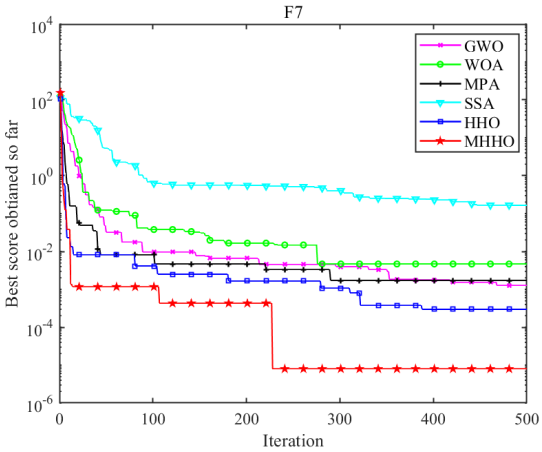
F7
Best score obtianed so far
Iteration
GWO
WOA
MPA
SSA
HHO
MHHO

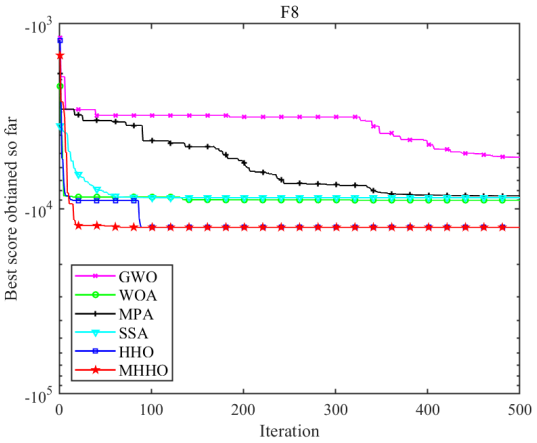
F8
Best score obtianed so far
Iteration
GWO
WOA
MPA
SSA
HHO
MHHO

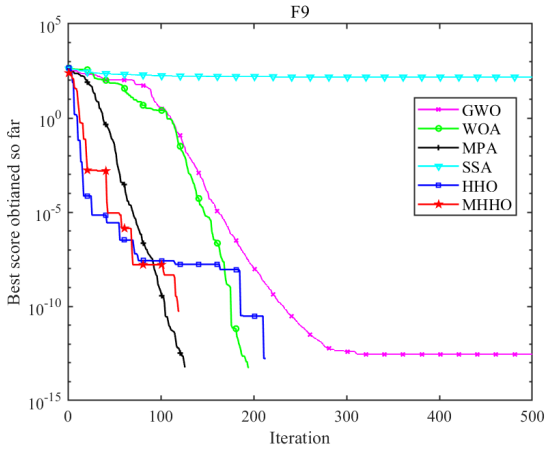
F9
Best score obtianed so far
Iteration
GWO
WOA
MPA
SSA
HHO
MHHO

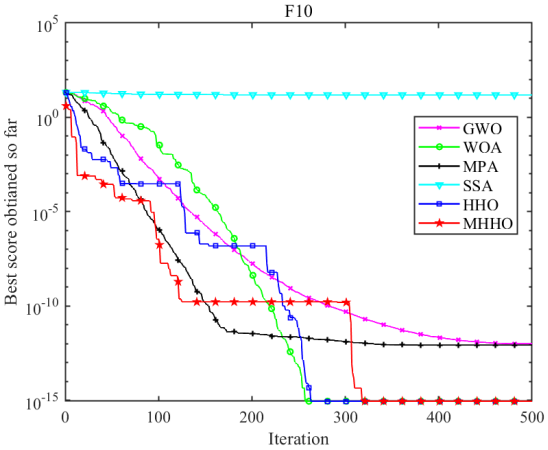
F10
Best score obtianed so far
Iteration
GWO
WOA
MPA
SSA
HHO
MHHO

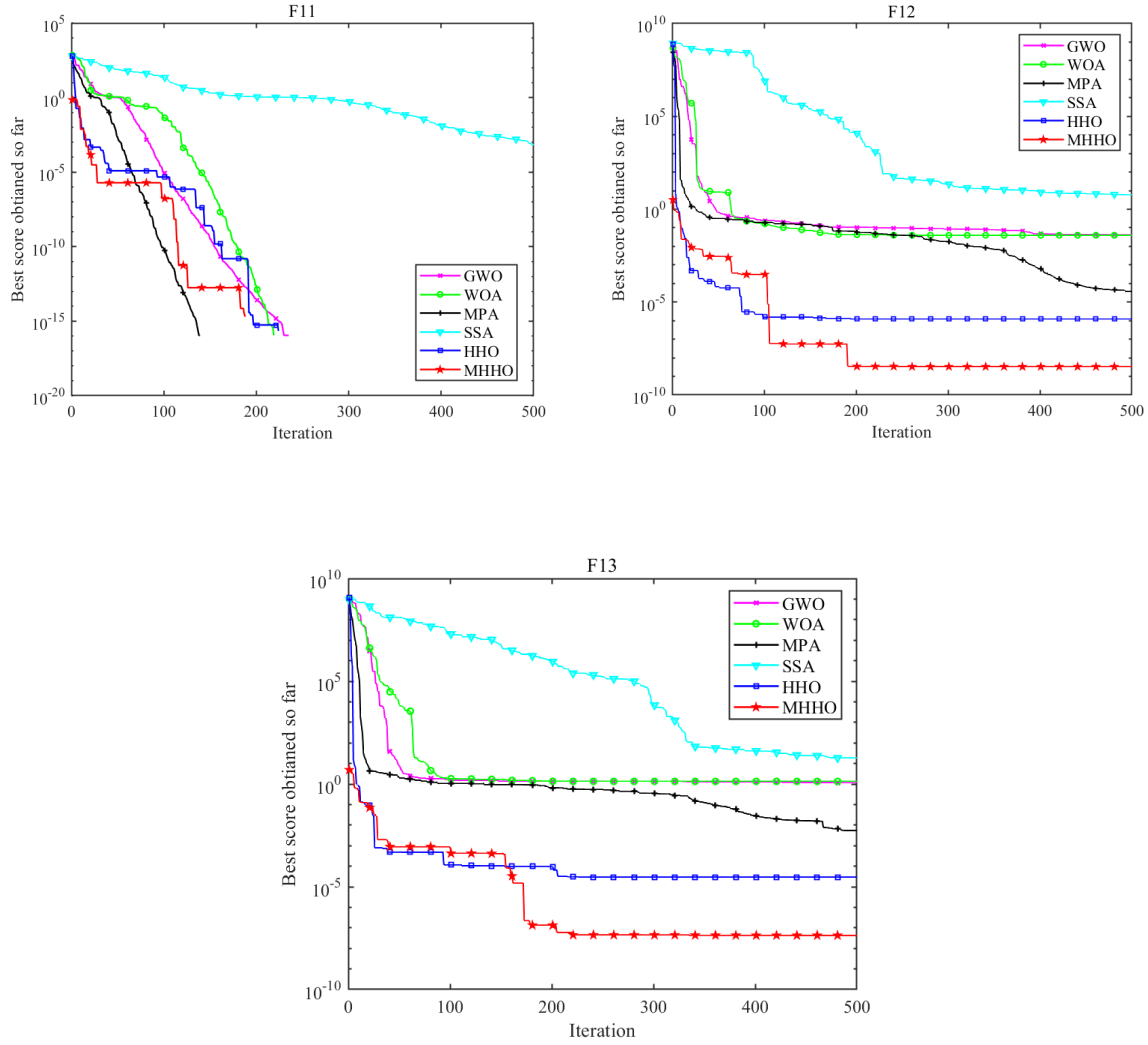

Fig. 3. The convergence curves of the MHHO and other algorithms

In Fig. 3, the convergence rate of the MHHO algorithm is significantly faster than other algorithms for functions F1~F7, F12, and F13. As shown in Table 2, the MHHO algorithm can achieve the optimal values of F1~F7, F12, and F13, which cannot be achieved by other algorithms. For function F8, although the optimal value obtained by the MHHO algorithm is equal to that that obtained by the HHO algorithm, the convergence rate of the MHHO algorithm is faster than the HHO algorithm. For functions F9 and F11, the convergence accuracy and convergence speed of the MHHO algorithm are better than those of the HHO algorithm. For function F10, the optimal value obtained by the MHHO algorithm is equal to the HHO algorithm, however, the convergence rate of the MHHO algorithm is slightly worse than the HHO algorithm.

4.3 Solving the Indoor 3D Visible Light Positioning Problem

A problem of indoor VLP is formulated and implemented to verify the optimization performance of the MHHO algorithm. The VLP system for a typical indoor environment is depicted in Fig. 4, where light-emitting diodes (LEDs) as signal generators, and a photodiode (PD) as the positioning terminal. Each LED light transmits the information which is modulated by the code division multiple access spreading code [37], and the PD receives and decodes the information. Because the information is related to the three-dimensional (3D) coordinates of the

LED, which can be represented as (X_i, Y_i, Z_i), i = 1, 2, 3, 4 for the four LEDs, the PD can use the coordinates of the LEDs to calculate the self-location [38, 39]. Consequently, the estimation of PD position in indoor VLP systems can be viewed as an optimization problem.

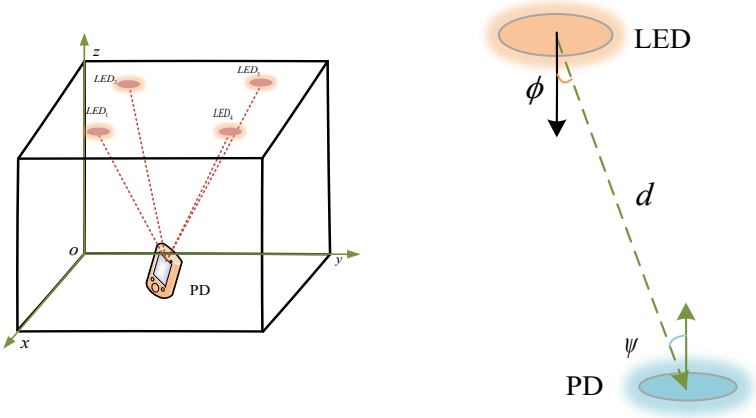

Fig. 4. The model of visible light positioning

Therefore, intelligent optimization algorithms are used for indoor positioning to search for the optimal position of the PD.

According to the model of the indoor VLP system, the direct current gain of the channel can be calculated as [27]:

$$H(0)_{LOS} = \begin{cases} \dfrac{(m+1)A}{2\pi d^2}\cos^m(\phi)T_s(\psi)g(\psi)\cos(\psi), & 0 \le \psi \le \psi_c \\ 0, & \psi > \psi_c \end{cases}, \tag{23}$$

where A represents the effective area of the PD, ϕ denotes the irradiation angle, ψ represents the angle of incidence, ψ_c denotes the field of view (FOV) of the PD, $T_s(\psi)$ and $g(\psi)$ represent the gain of the optical filter and the optical concentrator, respectively. d indicates the distance from the LED to the PD, and m denotes the Lambert parameter expressed as:

$$m = -\log 2 / \log(\cos(\phi_{1/2})), \tag{24}$$

where $\phi_{1/2}$ denotes the angle at half power of the LED.

Assuming that the transmitted power of the LED is P_t, and the received power of the PD is calculated as:

$$P_r = P_t \times H(0)_{LOS}. \tag{25}$$

The fitness function is represented by the receiver signal strength (RSS), calculated as [40]:

$$Fitness = \sum_{i=1}^{4}(P_r^i - \hat{P}_r^i)^2, \tag{26}$$

where P_r^i and $\hat{P}_r^i$ represent the RSS of the test point and the estimated point from the i-th LED, respectively.

In this section, the MHHO algorithm is used for the indoor VLP system to improve the positioning accuracy. The location of the PD can be obtained through the optimal search of the proposed algorithm, and the detailed procedures are summarized as follows:

Step1: The parameters setting.

The main setting parameters are shown in Table 3.

Table 3. Main setting parameters

Parameter	Value
The transmitter power of the LED, P_t	2.2 W
Coordinates of the four LEDs	[5,0,6], [0,0,6], [0,5,6], [5,5,6],
The effective area of the PD, A	1 cm^2
The half-power angle of LED, $\phi_{1/2}$	60°
FOV of the PD, ψ_c	90°
Refractive index, n	1.5
Population size, N_p	50
Variable dimension, D	3
Max iteration number, T	100

Step2: Initialization of the algorithm.

In the VLP system, a random position is generated in the solution space as the initial position of the optimized individual, and these initial positions are also the candidate positions of the PD. The fitness of each random individual position is calculated according to Eq. (26), and the best position of the individual is selected with the minimum fitness function.

Step3: Updating individual positions.

In this step, the individual positions are updated through two phases of the MMHO algorithm.

Step4: Termination judgment for algorithm optimization search.

When the number of iterations reaches the maximum, the algorithm search iteration is terminated. Otherwise, the algorithm continues to find the optimal position.

In this simulation, it was assumed that the PD of an indoor VLP system moved within the room, a spiral-shaped path was generated, and 158 points were selected uniformly as test points to the path.

The location results of the MHHO algorithm in the movement are shown in Fig. 5(a) to Fig. 5(d). As shown in Fig. 5(a) to Fig. 5(c), the blue line represents the movement path of the PD, and the red dots indicate the estimated point positions, which are very close to the actual path. Fig. 5(d) shows that an average 3D positioning error of 1.03 cm, a vertical positioning error of 0.74 cm, and a horizontal positioning error of 0.84 cm are achieved.

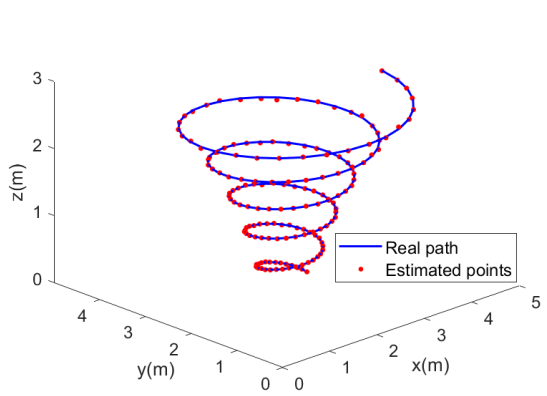

(a) The positioning results in a moving scene

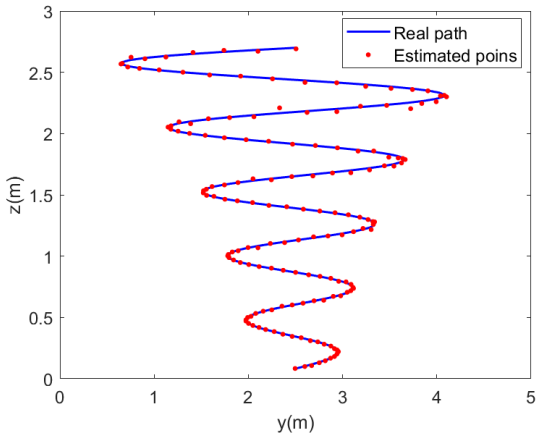

(b) Vertical view of the positioning result

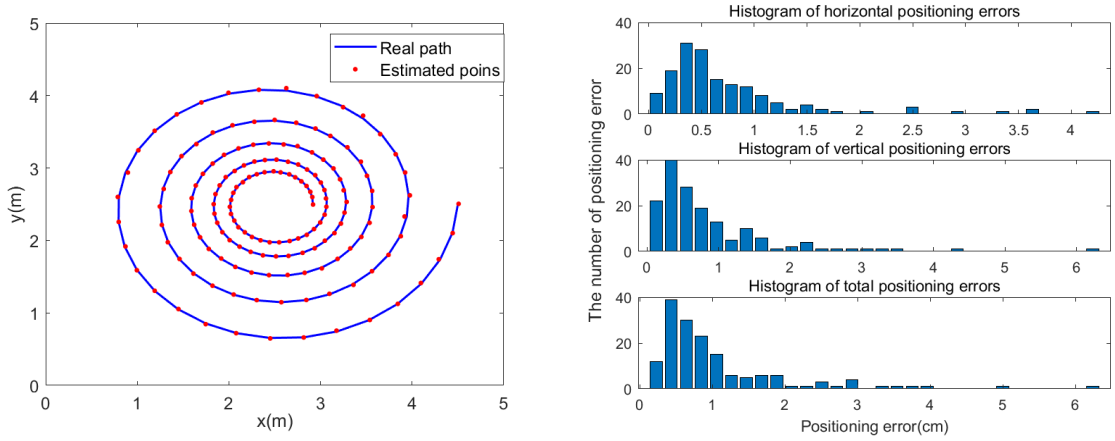

(c) Horizontal view of the positioning result (d) Histograms of positioning error

Fig. 5. Positioning results of the MHHO algorithm

The GWO, WOA, MPA, SSA, and HHO algorithms are simulated on the test points to further verify the proposed algorithm's effectiveness. The average, maximum, and minimum positioning errors achieved by the GWO, WOA, MPA, SSA, and HHO algorithms are listed in Table 4. From Table 4, the average positioning errors of the GWO, WOA, MPA, SSA, and HHO algorithms are 12.74 cm, 2.23 cm, 2.19 cm, 1.43 cm, and 1.57 cm, respectively. The experimental results show that the positioning accuracy of the MHHO algorithm is superior to other algorithms.

Table 4. Results of the indoor 3D visible light positioning

Algorithm	Average positioning error (cm)	Maximum positioning error (cm)	Minimum positioning error (cm)
GWO	12.74	25.40	3.61
WOA	2.23	15.87	0.23
MPA	2.19	9.16	0.10
SSA	1.43	7.57	0.36
HHO	1.57	10.15	0.25
MHHO	1.03	6.34	0.12

5 Conclusions

This paper presents a novel MHHO algorithm, which is combined with chaotic mapping, a nonlinear escape energy update strategy, and a nonlinear control strategy. The proposed algorithm applies the chaotic mapping to the population initialization to select an appropriate initiation position, which improves the HHO algorithm's search performance. Then, a nonlinear energy update strategy is presented to control the transformation of the algorithm phase, and the algorithm avoids getting trapped in a local optimum. Furthermore, a nonlinear control strategy is applied to further enhance the effectiveness of the HHO algorithm. The benchmark test functions are selected to verify the search performance of the MHHO algorithm. The experimental results show that the searching ability of the proposed algorithm is better than other intelligent algorithms. Finally, the MHHO algorithm is used to address the real problem of indoor 3D visible light positioning. Compared with other intelligent algorithms, the MHHO algorithm can obtain high localization accuracy, which proves that the MHHO algorithm is an effective way for indoor visible light positioning.

In future work, the effectiveness of the MHHO algorithm for indoor visible light localization will be verified using a robotic platform. In addition, the MHHO algorithm will be used for other practical engineering designs.

Acknowledgment

This research is supported by the Natural Science Research Project in Anhui Province University of China (Grant Nos. KJ2020A0636, KJ2021A1164, KJ2021A1165, 2022AH051669, and 2022AH051683), the Research Special Zone Project of West Anhui University (Grant No. 0044020001), and the Anhui Province University Quality Engineering Project of China (Grant No. 2020jyxm2146).

References

[1] R.A. Ibrahim, M.A. Elaziz, S. Lu, Chaotic opposition-based grey-wolf optimization algorithm based on differential evolution and disruption operator for global optimization, Expert Systems with Applications 108(2018) 1-27.
[2] Z. Wang, Q. Luo, Y. Zhou, Hybrid metaheuristic algorithm using butterfly and flower pollination base on mutualism mechanism for global optimization problems, Engineering with Computers 37(4)(2020) 3665-3698.
[3] S. Bharati, P. Podder, M.R.H. Mondal, Hybrid deep learning for detecting lung diseases from X-ray images, Inform Med Unlocked 20(2020) 100391.
[4] S. Gupta, K. Deep, A memory-based Grey Wolf Optimizer for global optimization tasks, Applied Soft Computing 93(2020) 106367.
[5] S. Duan, H. Luo, H. Liu, A.R. Prabowo, An Elastic Collision Seeker Optimization Algorithm for Optimization Constrained Engineering Problems, Mathematical Problems in Engineering 2022(2022) 1344667.
[6] S. Bharati, P. Podder, M.R.H. Mondal, V.B.S. Prasath, CO-ResNet: Optimized ResNet model for COVID-19 diagnosis from X-ray images, International Journal of Hybrid Intelligent Systems 17(1-2)(2021) 71-85.
[7] D. Whitley, A genetic algorithm tutorial, Statistics and Computing 4(2)(1994) 65-85.
[8] R. Storn, K. Price, Differential Evolution – A Simple and Efficient Heuristic for Global Optimization over Continuous Spaces, J. Global Optim 11(4) (1997) 341–359.
[9] D. Simon, Biogeography-Based Optimization, IEEE Transactions on Evolutionary Computation 12(6)(2008) 702-713.
[10] J. Kennedy, R. Eberhart. Particle swarm optimization. in Proceedings of ICNN'95 - International Conference on Neural Networks. 1995.
[11] M. Dorigo, M. Birattari, T. Stutzle, Ant colony optimization, IEEE Computational Intelligence Magazine 1(4)(2006) 28-39.
[12] X.S. Yang, D. Suash. Cuckoo Search via Lévy flights. in 2009 World Congress on Nature & Biologically Inspired Computing, 2009.
[13] S. Mirjalili, S.M. Mirjalili, A. Lewis, Grey Wolf Optimizer, Advances in Engineering Software 69(2014) 46-61.
[14] O. Hasançebi, T. Teke, O. Pekcan, A bat-inspired algorithm for structural optimization, Computers & Structures 128(2013) 77-90.
[15] S. Mirjalili, A. Lewis, The Whale Optimization Algorithm, Advances in Engineering Software 952016) 51-67.
[16] A. Faramarzi, M. Heidarinejad, S. Mirjalili, A.H. Gandomi, Marine Predators Algorithm: A nature-inspired metaheuristic, Expert Systems with Applications 152(2020) 113377.
[17] J. Xue, B. Shen, A novel swarm intelligence optimization approach: sparrow search algorithm, Systems Science & Control Engineering 8(1)(2020) 22-34.
[18] A.A. Heidari, S. Mirjalili, H. Faris, I. Aljarah, M. Mafarja, H. Chen, Harris hawks optimization: Algorithm and applications, Future Generation Computer Systems 97(2019) 849-872.
[19] İ. Çetinbaş, B. Tamyürek, M. Demirtaş, Sizing optimization and design of an autonomous AC microgrid for commercial loads using Harris Hawks Optimization algorithm, Energy Conversion and Management 245(2021) 114562.
[20] O. Akdag, A. Ates, C. Yeroglu, Modification of Harris hawks optimization algorithm with random distribution functions for optimum power flow problem, Neural Computing and Applications 33(6)(2020) 1959-1985.
[21] P. Du, J. Wang, Y. Hao, T. Niu, W. Yang, A novel hybrid model based on multi-objective Harris hawks optimization algorithm for daily PM2.5 and PM10 forecasting, Applied Soft Computing 96(2020) 106620.
[22] H. Chen, S. Jiao, M. Wang, A.A. Heidari, X. Zhao, Parameters identification of photovoltaic cells and modules using diversification-enriched Harris hawks optimization with chaotic drifts, Journal of Cleaner Production 244(2020) 118778.
[23] X. Bao, H. Jia, C. Lang, A Novel Hybrid Harris Hawks Optimization for Color Image Multilevel Thresholding Segmentation, IEEE Access 7(2019) 76529-76546.
[24] I. Attiya, M. Abd Elaziz, S. Xiong, Job Scheduling in Cloud Computing Using a Modified Harris Hawks Optimization and Simulated Annealing Algorithm, Comput Intell Neurosci 2020(2020) 3504642.
[25] C. Li, J. Li, H. Chen, M. Jin, H. Ren, Enhanced Harris hawks optimization with multi-strategy for global optimization tasks, Expert Systems with Applications 185(2021) 115499.
[26] Y. Wu, X. Liu, W. Guan, B. Chen, X. Chen, C. Xie, High-speed 3D indoor localization system based on visible light communication using differential evolution algorithm, Optics Communications 424(2018) 177-189.
[27] Y. Cai, W. Guan, Y. Wu, C. Xie, Y. Chen, L. Fang, Indoor High Precision Three-Dimensional Positioning System Based on Visible Light Communication Using Particle Swarm Optimization, IEEE Photonics Journal 9(6)(2017) 1-20.

[28] H. Turabieh, S.A. Azwari, M. Rokaya, W. Alosaimi, A. Alharbi, W. Alhakami, M. Alnfiai, Enhanced Harris Hawks optimization as a feature selection for the prediction of student performance, Computing 103(7)(2021) 1417-1438.
[29] E.H. Houssein, M.E. Hosney, M. Elhoseny, D. Oliva, W.M. Mohamed, M. Hassaballah, Hybrid Harris hawks optimization with cuckoo search for drug design and discovery in chemoinformatics, Sci Rep 10(1)(2020) 14439.
[30] N. Kardani, A. Bardhan, B. Roy, P. Samui, M. Nazem, D.J. Armaghani, A. Zhou, A novel improved Harris Hawks optimization algorithm coupled with ELM for predicting permeability of tight carbonates, Engineering with Computers, 2021.
[31] A.H. Gandomi, X.-S. Yang, Chaotic bat algorithm, Journal of Computational Science 5(2)(2014) 224-232.
[32] S. Arora, G. Kaur, Chaotic whale optimization algorithm, Journal of Computational Design and Engineering 5(3)(2018) 275-284.
[33] C. Paul, P.K. Roy, V. Mukherjee, Chaotic whale optimization algorithm for optimal solution of combined heat and power economic dispatch problem incorporating wind, Renewable Energy Focus 35(2020) 56-71.
[34] A.A. Dehkordi, A.S. Sadiq, S. Mirjalili, K.Z. Ghafoor, Nonlinear-based Chaotic Harris Hawks Optimizer: Algorithm and Internet of Vehicles application, Applied Soft Computing 109(2021) 107574.
[35] M. Khishe, M.R. Mosavi, Chimp optimization algorithm, Expert Systems with Applications 1492020).
[36] E. Rashedi, H. Nezamabadi-pour, and S. Saryazdi, GSA: A Gravitational Search Algorithm, Information Sciences 179(13)(2009) 2232-2248.
[37] H. Chen, W. Guan, S. Li, Y. Wu, Indoor high precision three-dimensional positioning system based on visible light communication using modified genetic algorithm, Optics Communications 413(2018) 103-120.
[38] S. Xu, Y. Wu, X. Wang, F. Wei, Indoor 3D visible light positioning system based on adaptive parameter particle swarm optimisation, IET Communications 14(20)(2020) 3707-3714.
[39] Y. Chen, H. Zheng, H. Liu, Z. Han, Z. Ren, Indoor High Precision Three-Dimensional Positioning System Based on Visible Light Communication Using Improved Hybrid Bat Algorithm, IEEE Photonics Journal 12(5)(2020) 1-13.
[40] C. Jia, T. Yang, C. Wang, M. Sun, High-Accuracy 3D Indoor Visible Light Positioning Method Based on the Improved Adaptive Cuckoo Search Algorithm, Arabian Journal for Science and Engineering 47(2)(2022) 2479-2498.